

Supplementary Information

Transport and accumulation of plasma generated species in aqueous solution

Christof C W Verlackt*, Wilma Van Boxem, Annemie Bogaerts*

Research group PLASMANT, University of Antwerp, Department of Chemistry, Universiteitsplein 1, 2610 Wilrijk, Belgium

*Corresponding author:

Christof.verlackt@uantwerpen.be

Annemie.bogaerts@uantwerpen.be (Lead contact)

Details on the Computational Setup

General equations in the model

In the model, three physical modules are coupled: transport of momentum, as well as the convection-diffusion equations for both heat and mass. For the transport of momentum, the incompressible Navier-Stokes equations are used:

$$\rho \nabla \cdot \vec{u} = 0$$

$$\rho(\vec{u} \cdot \nabla \vec{u}) = \nabla \left[-pI + \mu(\nabla \vec{u} + (\nabla \vec{u})^T) - \frac{2}{3}\mu(\nabla \cdot \vec{u})I \right]$$

These two expressions represent the conservation of mass and momentum, respectively. ρ is the overall mass density, \vec{u} the fluid velocity, μ the dynamic viscosity, p the static pressure, and I represents a unity matrix. Both ρ and μ are determined by the properties of the material (i.e. air and water in our case).

The equation for heat transport is based on the principle of conservation of energy and can be written as:

$$\rho C_p \left(\frac{\delta T}{\delta t} + \vec{u} \cdot \nabla T \right) = \nabla \cdot (k \nabla T) + Q$$

C_p is the heat capacity at constant pressure and k represents the thermal conductivity. Q stands for additional heat sources introduced to the system, such as the heat of evaporation (see later). The left side of the equation considers the changes in temperature as a function of time and due to convection. The first term on the right side represents the conductive heat flux.

The equation for mass transport used in this model is:

$$\frac{\delta c_i}{\delta t} + \nabla \cdot (-D_i \nabla c_i) + \vec{u} \cdot \nabla c_i = R_i$$

c_i and D_i represent the concentration and diffusion coefficient of each species i . R_i is the sum of all production and loss terms in the simulation, as described by chemical reactions. The left side of the equation represents changes in concentration as a function of time and due to diffusion (governed by D_i) and convection (cf. velocity \vec{u}).


Plasma species and chemistry

The gas phase species are introduced via the inlet at the very top of the plasma jet device (see Figure 1 in the main paper), with concentrations that will be specified below. The open boundaries of the model in the gas phase mimic the ambient air (78.09 % N₂, 20.95 % O₂ and 0.96 % H₂O) with a pressure of 1 atm. In this way, fresh air is introduced in the model when an inward flow is present, due to differences in pressure and concentration of the ambient air species. The walls of the liquid (cf. Figure 1 in main text) are treated with the non-slip condition, reducing the lateral velocity at the walls to 0 m.s⁻¹.

We don't consider the discharge (and the plasma chemistry) inside the plasma jet device in our model, because this would lead to excessive calculation times when using the model for actual plasma treatment times of several minutes, as explained in the main text. Therefore, we need the concentrations of the important species flowing out of the jet device as input in our model. They are adopted from Wende et al.¹ for the Ar plasma jet studied in this work. However, in practice, the gas phase species are introduced in our model through the inlet of the plasma jet device, as mentioned above. Therefore, we keep the concentrations of these species constant throughout the device, until they reach the nozzle, where the species interact with the ambient air and start to react with the air molecules. The inlet concentrations of the various species are listed in Table S.1.

The model considers 20 gas phase species and 22 liquid phase species (listed in the main paper), which react with each other in 57 gas phase reactions and 42 liquid phase reactions. These reactions, along with their rate coefficient and the references where these data are adopted from, are listed in Table S.2.

Boundary conditions at the interface

 The gas-liquid interface couples the three physical modules (see above) of both the gas and liquid phase by various boundary conditions. For the transport of momentum, drag from the gas phase is implemented on the interface, resulting in a shear stress in the liquid, which induces a flow in the liquid. In practice, this means that a moving wall is introduced in the model for the liquid at the interface, which has the lateral velocity of the gas at the other side of the interface, u_g . Furthermore, the gas velocity at the interface is reduced compared to the bulk gas flow, due to the presence of the interface, which is, again, treated as a moving wall with a lateral velocity of the liquid, u_l . In this way, the gas flow and liquid flow are coupled in the model through the interface.

Transport of heat over the interface is considered to be continuous and is controlled by the properties of the respective phases, i.e. thermal conductivity, heat capacity and specific heat ratio. In addition, the heat of water evaporation is introduced at the interface, which can affect the temperature of the liquid. This is included in the following way²:

$$Q = J_{z,H_2O} \cdot H_{vap}$$

Where J_{z,H_2O} is the molar flux of H₂O at the interface as a result of evaporation, and H_{vap} represents the latent heat of evaporation for water (set to be 2260 kJ/kg³).

For the transport of mass, two boundary conditions are applied. First, the transport of species over the interface is governed by Henry's law. This means that the concentrations of both the gas phase and liquid phase species are set to be in equilibrium with each other at the interface, by means of $c_{i, liquid} = c_{i, gas} * H_i * RT$, where H_i is the Henry's constant of species i , R the gas constant and T the temperature. The Henry's constants used in this model for the various species, as well as the diffusion constants of these species in the gas phase and liquid phase, are listed in Table S.3. In our model, we assume that only neutral species are able to enter the gas phase from the liquid, while ions will remain in the liquid phase.

The second boundary condition for transport of mass at the gas-liquid interface is given by water evaporation. This is included via the water vapor pressure at the interface in the gas phase as follows⁴:

$$\log_{10} p_{vap} = 8.07131 - \frac{1730.63}{233.426 + T}$$

p_{vap} represents the vapor pressure of water and T the temperature. The constants in the equation are known as Antoine's coefficients, which are material specific. The constants in this equation are the Antoine's coefficients for liquid water⁴.

Table S.1 shows gaseous species number densities in cm^{-3} at the inlet of the plasma jet device. They serve as input data for the calculation of the gas phase and have been adopted from¹ for an Ar plasma jet. Species that are not included in this table are assumed to have a zero inlet concentration.

Species	Inlet concentration	Species	Inlet concentration
OH	2×10^{14}	H	1×10^{15}
H₂O₂	1×10^{13}	N	6×10^{13}
HO₂	3×10^{13}	NO	7×10^{13}
O	1×10^{15}	NO₂	1×10^{12}
O₃	7×10^{11}	HNO₂	2×10^{12}
¹O₂	2×10^{14}	HNO₃	2×10^{10}
H₂	4×10^{11}	Ar	2×10^{19}

Table S1 Reaction list with all gas phase and liquid phase reactions included in the model, as well as the rate coefficients (or the data to calculate the rate coefficients) and the references where these data were adopted from. The rate coefficients for the gas phase reactions are given in the Arrhenius form: $k = A \times (T_g/300)^B \times \exp(-C/T_g)$, with units of s^{-1} , cm^3s^{-1} and cm^6s^{-1} for first, second and third order reactions. The unit of A is the same as for k, B is dimensionless, and the unit of C and T_g is K. The unit for the liquid phase rate coefficients is s^{-1} , $m^3mol^{-1}s^{-1}$ and $m^6mol^{-2}s^{-1}$ for first, second and third order reactions, respectively.

Nr	Reaction	Reaction rate coefficient			Ref.
		A	B	C	
Gas phase reactions					
1	$O + OH \rightarrow H + O_2$	1.81×10^{-11}	-0.31	-177	5
2	$O + O_2 + M \rightarrow O_3 + M$	6.40×10^{-35}	0	-663	5
3	$O + NO_2 \rightarrow NO + O_2$	6.50×10^{-12}	0	-120	5
4	$O + O_3 \rightarrow O_2 + O_2$	8.00×10^{-12}	0	2060	5
5	$O + O_3 \rightarrow {}^1O_2 + O_2$	1.00×10^{-11}	0	2300	5
6	$O + O + M \rightarrow {}^1O_2 + M$	6.93×10^{-35}	-0.63	0	6
7	$O + HO_2 \rightarrow OH + O_2$	2.71×10^{-11}	0	-224	5
8	$O + NO + M \rightarrow NO_2 + M$	1.00×10^{-31}	-1.6	0	5
9	$O + NO_3 \rightarrow NO_2 + O_2$	1.70×10^{-11}	0	0	5
10	$O + O + M \rightarrow O_2 + M$	5.21×10^{-35}	0	-900	5
11	$O + N + M \rightarrow NO + M$	1.02×10^{-32}	-0.5	0	5
12	$O + HNO_3 \rightarrow OH + NO_3$	3.00×10^{-17}	0	0	5
13	$O + NO_2 + M \rightarrow NO_3 + M$	9.00×10^{-32}	-2	0	5
14	$O + H_2O_2 \rightarrow HO_2 + OH$	1.79×10^{-13}	2.92	1394	5
15	$O + H_2O_2 \rightarrow H_2O + O_2$	1.45×10^{-15}	0	0	5
16	$O + HNO_2 \rightarrow OH + NO_2$	2.00×10^{-11}	0	3000	5
17	$O_2 + NO_3 \rightarrow NO_2 + O_3$	1.00×10^{-17}	0	0	5
18	$O_2 + {}^1O_2 \rightarrow O_3 + O$	3.00×10^{-21}	0	0	6
19	${}^1O_2 + M \rightarrow O_2 + M$	3.00×10^{-18}	0	200	5
20	${}^1O_2 + HO_2 \rightarrow OH + O_2 + O$	1.66×10^{-11}	0	0	5
21	${}^1O_2 + O_3 \rightarrow O_2 + O_2 + O$	1.00×10^{-14}	0	0	5
22	$O_3 + NO \rightarrow NO_2 + O_2$	4.30×10^{-12}	0	1560	5
23	$O_3 + NO_2 \rightarrow NO_3 + O_2$	1.40×10^{-13}	0	2470	5
24	$O_3 + OH \rightarrow HO_2 + O_2$	1.69×10^{-12}	0	941	5
25	$O_3 + HNO_2 \rightarrow HNO_3 + O_2$	5.00×10^{-19}	0	0	6
26	$O_3 + O_3 \rightarrow {}^1O_2 + O_2 + O_2$	1.00×10^{-11}	0	2300	5
27	$O_3 + H \rightarrow OH + O_2$	2.71×10^{-11}	0.75	0	5
28	$OH + NO_2 + M \rightarrow HNO_3 + M$	4.60×10^{-29}	-5.49	1180	5
29	$OH + NO + M \rightarrow HNO_2 + M$	7.40×10^{-31}	-2.4	0	5

30	$\text{OH} + \text{H}_2\text{O}_2 \rightarrow \text{H}_2\text{O} + \text{HO}_2$	4.53×10^{-12}	0	288.9	5
31	$\text{OH} + \text{OH} \rightarrow \text{H}_2\text{O} + \text{O}$	5.49×10^{-14}	2.42	-970	5
32	$\text{OH} + \text{HO}_2 \rightarrow \text{H}_2\text{O} + \text{O}_2$	4.80×10^{-11}	0	-250	5
33	$\text{OH} + \text{HNO}_2 \rightarrow \text{H}_2\text{O} + \text{NO}_2$	2.70×10^{-12}	0	-260	5
34	$\text{OH} + \text{OH} + \text{M} \rightarrow \text{H}_2\text{O}_2 + \text{M}$	8.00×10^{-31}	-0.8	0	5
35	$\text{OH} + \text{HNO}_3 \rightarrow \text{H}_2\text{O} + \text{NO}_3$	1.50×10^{-13}	0	0	5
36	$\text{HO}_2 + \text{NO} + \text{M} \rightarrow \text{HNO}_3 + \text{M}$	5.60×10^{-33}	0	0	5
37	$\text{HO}_2 + \text{NO} \rightarrow \text{NO}_2 + \text{OH}$	3.60×10^{-12}	0	-270	6
38	$\text{HO}_2 + \text{HO}_2 + \text{M} \rightarrow \text{H}_2\text{O}_2 + \text{O}_2 + \text{M}$	1.70×10^{-33}	0	-999.5	6
39	$\text{HO}_2 + \text{N} \rightarrow \text{NO} + \text{OH}$	2.20×10^{-11}	0	0	5
40	$\text{H} + \text{O}_2 + \text{M} \rightarrow \text{HO}_2 + \text{M}$	6.09×10^{-32}	-0.8	0	5
41	$\text{H} + \text{OH} + \text{M} \rightarrow \text{H}_2\text{O} + \text{M}$	8.00×10^{-31}	-2.6	0	5
42	$\text{H} + \text{HO}_2 \rightarrow \text{H}_2 + \text{O}_2$	2.06×10^{-11}	0.84	277	5
43	$\text{H} + \text{H}_2\text{O}_2 \rightarrow \text{H}_2\text{O} + \text{OH}$	4.00×10^{-11}	0	2000	5
44	$\text{H} + \text{HNO}_2 \rightarrow \text{H}_2 + \text{NO}_2$	2.00×10^{-11}	0	3700	5
45	$\text{H} + \text{NO}_3 \rightarrow \text{NO}_2 + \text{OH}$	5.80×10^{-10}	0	750	5
46	$\text{H} + \text{HO}_2 \rightarrow \text{OH} + \text{OH}$	1.66×10^{-10}	0	413	5
47	$\text{H} + \text{NO}_2 \rightarrow \text{OH} + \text{NO}$	4.00×10^{-10}	0	340	5
48	$\text{H}_2 + \text{OH} \rightarrow \text{H}_2\text{O} + \text{H}$	9.54×10^{-13}	2	1490	5
49	$\text{N} + \text{O}_2 \rightarrow \text{NO} + \text{O}$	3.30×10^{-12}	-1	3150	5
50	$\text{N} + \text{NO} \rightarrow \text{N}_2 + \text{O}$	8.20×10^{-11}	0	-410	5
51	$\text{N} + \text{NO}_3 \rightarrow \text{NO}_2 + \text{NO}$	3.00×10^{-12}	0	0	5
52	$\text{N} + \text{OH} \rightarrow \text{H} + \text{NO}$	4.70×10^{-11}	0	0	5
53	$\text{N} + \text{N} + \text{M} \rightarrow \text{N}_2 + \text{M}$	1.38×10^{-34}	0	0	5
54	$\text{N} + \text{NO}_2 \rightarrow \text{NO} + \text{NO}$	1.33×10^{-12}	0	-220	5
55	$\text{NO}_3 + \text{NO} \rightarrow \text{NO}_2 + \text{NO}_2$	1.80×10^{-11}	0	-110	5
56	$\text{NO}_3 + \text{NO}_2 + \text{M} \rightarrow \text{N}_2\text{O}_5 + \text{M}$	2.80×10^{-30}	-3.5	0	5
57	$\text{N}_2\text{O}_5 + \text{M} \rightarrow \text{NO}_2 + \text{NO}_3 + \text{M}$	1.33×10^{-3}	-3.5	11000	5
Liquid phase reactions		k			Ref.
58	$\text{H} + \text{H}_2\text{O} \rightarrow \text{H}_2 + \text{OH}$	1.00×10^{-2}			7
59	$\text{H} + \text{H} \rightarrow \text{H}_2$	7.50×10^6			7
60	$\text{H} + \text{OH} \rightarrow \text{H}_2\text{O}$	7.00×10^6			7
61	$\text{H} + \text{H}_2\text{O}_2 \rightarrow \text{OH} + \text{H}_2\text{O}$	9.00×10^4			7
62	$\text{H} + \text{O}_2 \rightarrow \text{HO}_2$	2.10×10^7			7
63	$\text{H} + \text{HO}_2 \rightarrow \text{H}_2\text{O}_2$	1.00×10^7			7

64	$\text{H} + \text{NO}_2 \cdot \rightarrow \text{OH} \cdot + \text{NO}$	1.20×10^6	7
65	$\text{H} + \text{NO}_2 \rightarrow \text{HNO}_2$	1.00×10^7	7
66	$\text{O} + \text{H}_2\text{O} \rightarrow \text{OH} + \text{OH}$	1.30×10^1	7
67	$\text{O} + \text{O}_2 \rightarrow \text{O}_3$	3.00×10^6	7
68	$\text{O}_2 \cdot + \text{NO} \rightarrow 0.7(\text{NO}_3 \cdot) + 0.3(\text{ONOO} \cdot)$	1.20×10^7	7
69	$\text{O}_3 + \text{O}_3 + \text{OH} \cdot \rightarrow \text{O}_2 + \text{O}_2 + \text{HO} + \text{O}_2 \cdot$	2.10×10^{-1}	8
70	$\text{O}_3 + \text{NO}_2 \cdot \rightarrow \text{O}_2 + \text{NO}_3 \cdot$	3.30×10^2	8
71	$\text{OH} + \text{OH} \rightarrow \text{H}_2\text{O}_2$	1.00×10^7	7
72	$\text{OH} + \text{H}_2 \rightarrow \text{H} + \text{H}_2\text{O}$	4.20×10^4	7
73	$\text{OH} + \text{HO}_2 \rightarrow \text{H}_2\text{O} + \text{O}_2$	6.00×10^6	7
74	$\text{OH} + \text{O}_2 \cdot \rightarrow \text{OH} \cdot + \text{O}_2$	8.00×10^6	7
75	$\text{OH} + \text{H}_2\text{O}_2 \rightarrow \text{H}_2\text{O} + \text{HO}_2$	2.70×10^4	7
76	$\text{OH} + \text{NO}_2 \cdot \rightarrow \text{OH} \cdot + \text{NO}_2$	1.00×10^7	7
77	$\text{HO}_2 + \text{H}_2\text{O} + \text{O}_2 \cdot \rightarrow \text{O}_2 + \text{H}_2\text{O}_2 + \text{OH} \cdot$	9.68×10^1	8
78	$\text{H}_2\text{O}_2 + \text{NO}_2 \cdot + \text{H}^+ \rightarrow \text{ONOOH} + \text{H}_2\text{O}$	1.1×10^{-3}	9
79	$\text{NO} + \text{NO} + \text{O}_2 \rightarrow \text{NO}_2 + \text{NO}_2$	2.30	7
80	$\text{NO} + \text{NO}_2 + \text{H}_2\text{O} \rightarrow \text{HNO}_2 + \text{HNO}_2$	2.00×10^2	7
81	$\text{NO} + \text{OH} \rightarrow \text{HNO}_2$	2.00×10^7	7
82	$\text{NO} + \text{O}_2 \cdot \rightarrow \text{NO}_3 \cdot$	8.00×10^6	7
83	$\text{NO} + \text{O}_2 \cdot \rightarrow \text{ONOO} \cdot$	3.20×10^6	7
84	$\text{NO}_2 + \text{OH} \rightarrow 0.7(\text{NO}_3 \cdot + \text{H}^+) + 0.3(\text{ONOOH})$	5.30×10^6	7
85	$\text{NO}_2 + \text{NO}_2 + \text{H}_2\text{O} \rightarrow \text{HNO}_2 + \text{H}^+ + \text{NO}_3 \cdot$	1.50×10^2	7
86	$\text{NO}_3 + \text{OH} \cdot \rightarrow \text{OH} + \text{NO}_3 \cdot$	8.00×10^4	8
87	$\text{N}_2\text{O}_5 + \text{H}_2\text{O} \rightarrow \text{NO}_3 \cdot + \text{NO}_3 \cdot + \text{H}^+ + \text{H}^+$	1.20×10^{-3}	7
88	$\text{HNO}_2 + \text{HNO}_2 \rightarrow \text{NO} + \text{NO}_2 + \text{H}_2\text{O}$	1.34×10^1	10
89	$\text{ONOOH} \rightarrow \text{NO}_3 \cdot + \text{H}^+$	1.20	11
90	$\text{ONOOH} \rightarrow \text{OH} + \text{NO}_2$	3×10^{-1}	11
91	$\text{ONOO} \cdot \rightarrow \text{NO} + \text{O}_2 \cdot$	2×10^{-2}	11
92	$\text{HO}_2 + \text{HO}_2 \rightarrow \text{O}_2 + \text{H}_2\text{O}_2$	8.3×10^2	8
93	$\text{H}_2\text{O}_2 + \text{O}_3 + \text{OH} \cdot \rightarrow \text{OH} + \text{HO}_2 + \text{O}_2 + \text{OH} \cdot$	$5.5 \times 10^{3-Z}$ $Z = 11.6 - \text{pH}$	12
94	$\text{OH} + \text{ONOO} \cdot \rightarrow \text{OH} \cdot + \text{O}_2 + \text{NO}$	4.8×10^6	13
95	$\text{NO}_3 + \text{H}_2\text{O}_2 \rightarrow \text{NO}_3 \cdot + \text{HO}_2 + \text{H}^+$	1.00×10^3	13
96	$\text{NO}_3 + \text{O}_2 \cdot \rightarrow \text{NO}_3 \cdot + \text{O}_2$	1.00×10^6	13
97	$\text{NO}_3 + \text{NO}_2 \cdot \rightarrow \text{NO}_3 \cdot + \text{NO}_2$	1.2×10^6	13

98	$O_3 + OH \rightarrow O_2 + HO_2$	1.00×10^5	8
98	$H_2O \rightarrow H^+ + OH^\cdot$	7×10^{-2}	10
99	$H^+ + OH^\cdot \rightarrow H_2O$	7×10^6	10
100	$HNO_2 \leftrightarrow H^+ + NO_2^\cdot$	pKa = 3.4	
101	$ONOOH \leftrightarrow H^+ + ONOO^\cdot$	pKa = 6.8	
102	$HO_2 \leftrightarrow H^+ + O_2^\cdot$	pKa = 4.88	



Table S.5. Diffusion constants used in the gas phase ($D_{i,gas}$) and liquid phase ($D_{i,liquid}$) and Henry constants (H_i) used in the model for the various species i , as well as the references where these data are adopted from. Species that do not have a value for $D_{i,gas}$ or $D_{i,liquid}$ are not considered in the gas or liquid phase, respectively.

Species	$D_{i,gas}$ $10^{-5} \text{ m}^2 \cdot \text{s}^{-1}$	Ref.	$D_{i,liquid}$ $10^{-9} \text{ m}^2 \cdot \text{s}^{-1}$	Ref.	H_i $\text{mol} \cdot \text{L}^{-1} \cdot \text{atm}^{-1}$	Ref.
Ar	12.2	14				
O ₂	2.1	14	2.3	10	1.3×10^{-3}	15
N ₂	2.1	14	2.6	16	6.5×10^{-4}	15
H ₂	12.2	14	1	10	7.8×10^{-4}	
H ₂ O	2.3	14	2.299	17		
OH	4	14	2.8	10	3.03×10^1	15
H ₂ O ₂	2	14	1.7	10	7.9×10^4	15
HO ₂	2	14	1.7	same as H ₂ O ₂	5.56×10^3	15
O	3.2	14	2.8	same as OH	1.3×10^{-3}	same as O ₂
O ₃	1.5	14	1.76	18	1.22×10^{-2}	15
¹ O ₂	2.1	14				
H	12.2	14	1	10	7.8×10^{-4}	same as H ₂
N	2.9	14				
NO	2	14	2.2	10	1.9×10^{-3}	15
NO ₂	1.7	14	1.85	10	1.93×10^{-2}	15
NO ₃	0.9	14	2.5	same as HNO ₃	3.28	15
HNO ₂	2.1	14	2.5	10	4.9×10^{-1}	15
HNO ₃	2.1	14	2.5	10	1.7×10^6	15
N ₂ O ₅	1	14	1	19	2.1	15
ONOOH	1.78	14	2.5	10	4.8×10^6	10
H ⁺			7	10		
OH ⁻			5.29	10		
O ₂ ⁻			2.3	estimated		
NO ₂ ⁻			1.7	10		
NO ₃ ⁻			1.7	10		
ONOO ⁻			1.7	same as NO ₃ ⁻		

Results and discussion

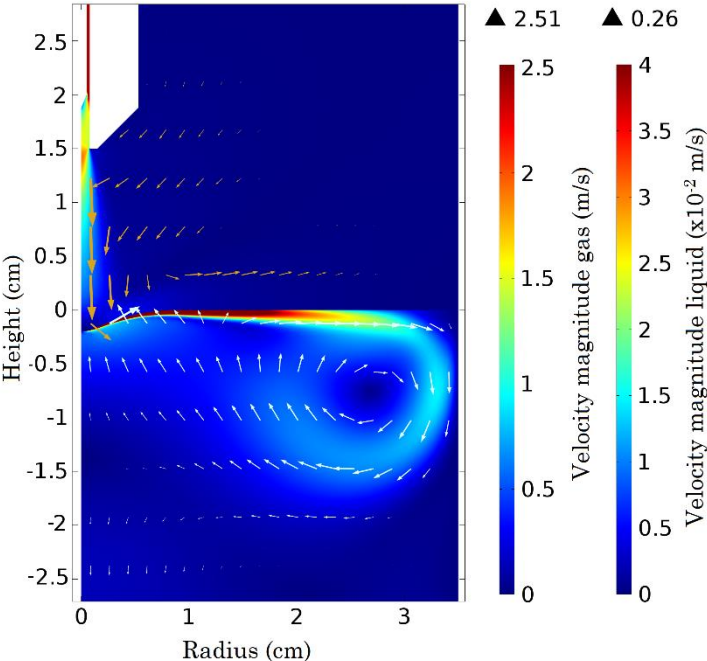


Figure S10: 2D plot of the velocity magnitude (depicted in rainbow color scale) in both gas and liquid phase, at an inlet gas flow rate of 0.1 slm. The direction of the flow is indicated by yellow and white arrows for the gas and liquid phase, respectively. The arrows are logarithmically scaled based on the velocity magnitude, for the sake of clarity. The symmetry axis is located at radius = 0 cm. The values above the color scale indicate the highest velocity in both gas and liquid phase (in m/s).

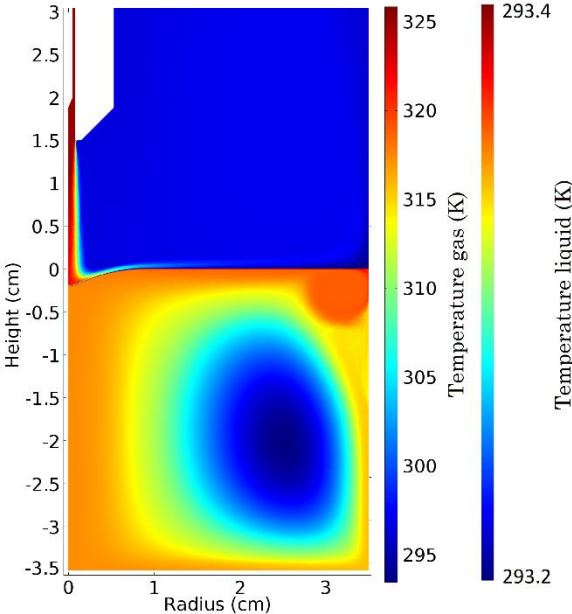


Figure S11: 2D plot of the temperature in both the gas and liquid phase presented in rainbow scale when heat of evaporation is disabled.

References

1. Wende, K. *et al.* Identification of the biologically active liquid chemistry induced by a nonthermal atmospheric pressure plasma jet. *Biointerphases* **10**, 29518 (2015).
2. Bird, R. B., Stewart, W. E. & Lightfoot, E. N. *Transport Phenomena*. (John Wiley & Sons, 2007).
3. Datt, P. in *Encyclopedia of Snow, Ice and Glaciers* (eds. Singh, V. P., Singh, P. & Haritashya, U. K.) 703 (Springer Netherlands, 2011). doi:10.1007/978-90-481-2642-2_327
4. Antoine, M. C. Tensions des vapeurs: nouvelle relation entre les tensions et les températures. *Comptes Rendus des Séances l'Académie des Sci.* **107**, 836–837 (1888).
5. Van Gaens, W. & Bogaerts, A. Kinetic modelling for an atmospheric pressure argon plasma jet in humid air. *J. Phys. D. Appl. Phys.* **46**, 275201 (2013).
6. Schmidt-Bleker, A., Winter, J., Bösel, A., Reuter, S. & Weltmann, K.-D. On the plasma chemistry of a cold atmospheric argon plasma jet with shielding gas device. *Plasma Sources Sci. Technol.* **25**, 15005 (2016).
7. Tian, W. & Kushner, M. J. Atmospheric pressure dielectric barrier discharges interacting with liquid covered tissue. *J. Phys. D. Appl. Phys.* **47**, 165201 (2014).
8. NIST Solution Kinetics Database. at <<http://kinetics.nist.gov/solution/>>
9. Lukes, P., Dolezalova, E., Sisrova, I. & Clupek, M. Aqueous-phase chemistry and bactericidal effects from gaseous plasmas in contact with water. *Plasma Sources Sci. Technol.* **23**, 15019 (2014).
10. Lindsay, A., Anderson, C., Slikboer, E., Shannon, S. & Graves, D. Momentum, heat, and neutral mass transport in convective atmospheric pressure plasma-liquid systems and implications for aqueous targets. *J. Phys. D. Appl. Phys.* **48**, 424007 (2015).
11. Loegager, T. & Sehested, K. Formation and Decay of Peroxynitric Acid: A Pulse Radiolysis Study. *J. Phys. Chem.* **97**, 10047–10052 (1993).
12. Staehelin, J. & Hoigné, J. Decomposition of Ozone in Water: Rate of Initiation by Hydroxide Ions and Hydrogen Peroxide. *Environ. Sci. Technol.* **16**, 676–681 (1982).
13. Liu, Z. C. *et al.* Physicochemical processes in the indirect interaction between surface air plasma and deionized water. *J. Phys. D. Appl. Phys.* **48**, 495201 (2015).
14. Sakiyama, Y., Graves, D. B., Chang, H.-W., Shimizu, T. & Morfill, G. E. Plasma chemistry model of surface microdischarge in humid air and dynamics of reactive neutral species. *J. Phys. D. Appl. Phys.* **45**, 425201 (2012).
15. Sander, R. Compilation of Henry's Law Constants for Inorganic and Organic Species of Potential Importance in Environmental Chemistry. (Max-Planck Institute of Chemistry, 1999).
16. Wise, D. L. & Houghton, G. Diffusion coefficients of neon, krypton, xenon, carbon monoxide and nitric oxide in water at 10–60°C. *Chem. Eng. Sci.* **23**, 1211–1216 (1968).
17. Holz, M., Heil, S. & Sacco, A. Temperature-dependent self-diffusion coefficients of water and six selected molecular liquids for calibration in accurate ¹H NMR PFG measurements. *Phys. Chem. Chem. Phys.* **2**, 4740–4742 (2000).

18. Johnson, P. N. & Davis, R. A. Diffusivity of Ozone in Water. *J. Chem. Eng. Data* **41**, 1485–1487 (1996).
19. Stewart, D. J., Griffiths, P. T. & Cox, R. A. and Physics Reactive uptake coefficients for heterogeneous reaction of N₂O₅ with submicron aerosols of NaCl and natural sea salt. *Atmos. Chem. Phys.* **4**, 1381–1388 (2004).